Grid Modernization: Seamless Integration of Protection, Optimization& Control

A. P. Sakis Meliopoulos
George J. Cokkinides
Georgia Tech
sakis.m@gatech.edu

Renke Huang
Evangelos Polymeneas
Georgia Tech
rhuang6@gatech.edu

Paul Myrda
Electric Power Research Institute (EPRI)
pmyrda@epri.com

Abstract

The objectives of smart grid and grid modernization are to increase automation and seamlessly integrate data, models, protection, optimization and control of the power grid. This effort is affected by technological advances. One such technology is the numerical relay which has increased its domination to the point that today has almost completely displaced electromechanical and solid state relays and the most recent technology of merging units that has separated the data acquisition function from protective relays and SCADA systems. The capabilities of the numerical relays are not fully utilized today; specifically, by and large, they simply mimic the logics that were developed for the electromechanical relays but with much more flexibility. Recent developments towards substation automation are utilizing the numerical relays for SCADA, communications and in general an integrated system for protection and control. These approaches indicate the recognition that numerical relays offer much more than simply mimicking protection functions of the past. They also offer the ability to form the basic infrastructure towards a fully automated power system, the subject of this paper.

In previous work, we presented a new protection scheme that is a generalization of differential protection. The approach is based on dynamic state estimation. Specifically, the protection scheme is based on continuously monitoring terminal voltages and currents of the component and other possible quantities such as tap setting, temperature, etc. as appropriate for the component under protection. The monitored data are utilized in a dynamic state estimation that continuously provides the dynamic state of the component. The dynamic state is then used to determine the health of the component. Tripping or no tripping is decided on the basis of the health of the component.

The present paper takes the above concept one step further. Using the dynamic state estimation of a protection zone as the basic technology, it builds an integrated automation system that performs the protection functions, validates models, transmits the models to the control center, integrates monitoring and control, enables optimization and provides automated disturbance playback capabilities. The system provides the infrastructure and real time models for any application along the spatial extend of the power system.

1. Introduction

The changing face of the electric power system due to new power apparatus and the proliferation of customer owned resources and smart devices calls for new approaches for protection, control and operation of the emerging electric power system. The emerging system requires better protection, more integration and more automation [1-2]. Better protection is required as we deal with systems with power electronic interfaces that limit fault currents to levels comparable to load currents; a fact that makes the traditional protection approaches obsolete. The integrated and automated system can take advantage of the combination of utility and customer resources to make the operation efficient (loss minimization, load levelization, etc.) and to improve the reliability of the system by responding in cases of need.

This paper proposes an infrastructure of data acquisition systems that provide the necessary information for an automated system that enables autonomous protection, model validation, a distributed state estimation and an integrated system of applications. The details of this system are given below.

2. Proposed Approach

The overall proposed structure is shown in Figure 1. The system starts from the relays that monitor power apparatus (a protection zone) and performs

978-1-4799-2504-9/14 $31.00 © 2014 IEEE
DOI 10.1109/HICSS.2014.309

dynamic state estimation at the apparatus level. The dynamic state estimation is performed a few thousand times per second depending on the sampling period of the data acquisition systems. For example, if the relay samples 4000 times per second, the dynamic state estimation is executed 2000 times per second (or within 500 microseconds). The code has been optimized and as an example the computations of the dynamic state estimation for a transmission line can be performed within 30 microseconds in a high end personal computer. This process is described in the section setting-less protection and it has been demonstrated with extensive numerical experiments and in the laboratory [3-7]. The indicated relay is a numerical relay on which a number of new functions have been added. We will refer to this relay as Universal Monitoring Protection and Control Unit (UMPCU) [8]. The UMPCU provides the real time model of the component, estimated measurements and status of connectivity of the component at very fast speeds. These results are used to perform component protection (setting-less protection) [9]. The results of the dynamic state estimation over a period of one cycle are used to compute the state of the component in the "phasor domain", see block "Conversion to Phasor Model". These results include the following information for the power apparatus (protection zone): ((1) connectivity, (2) device model, (3) measurements, and (4) controls). Subsequently, this information is used to synthesize the substation state as shown in Figure 1. Note that the substation state is updated once per cycle. Finally the substation state is transmitted to the control center where the system state is synthesized. Note that the synthesis of the substation state as well as the synthesis of the system state at the control center, does not require additional computations since the component models are all in UTC time (due to the GPS synchronized measurements) and therefore they can be simply merged to provide the system wide model.

It should be stressed that the functional specifications of the UMPCU can be met by current top-of-the-line numerical protective relays. Specifically, the computational power of these relays is adequate to perform the analytics of the UMPCU, i.e. the state estimation based protection function and the extraction of the real time model of the component by appropriate programming. The UMPCUs are also able to receive commands from the control center and apply them to control power apparatus just as present relays are able to do.We will like to point out that relay manufacturers do not allow access to their software and subsequent user modifications. For this reason, the laboratory implementation of this relay is a high end personal computer which is less expensive than a high end numerical relay.

It is emphasized that the proposed approach facilitates efficient communications. Specifically, each substation sends to the EMS only its real time model which comprises a very small number of data (for example for a typical substation about 40 to 50 variables fully describe the state of the substation). When connectivity changes, then connectivity data are transmitted by exception. Similarly if model changes occur, the new mathematical model will be transmitted by exception. The end result is that while the instrumentation may be collecting data at rates of hundreds of thousands of data points per second, the frequency domain state (phasors) are only a few tens of data points per cycle. Only the frequency domain component state is transmitted to the EMS.

The constituent parts of this approach are described next.

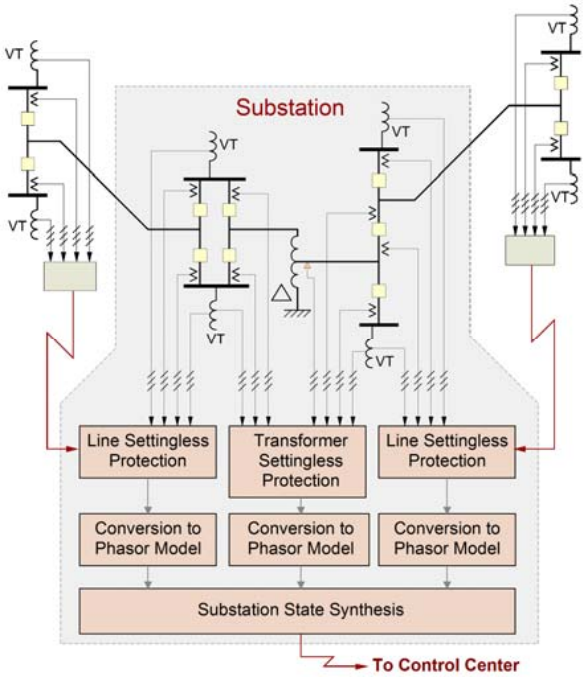

Figure 1: Illustration of overall approach

3. Zone Protection and Model Validation

For more secure protection of power components such as transmission lines, transformers, capacitor banks, motors, generators, etc., a new method has been developed that continuously monitor the dynamic model of the component under protection via dynamic state estimation. Specifically, the proposed method extracts the dynamic model of the

component under protection via dynamic state estimation [3-7]. The dynamic model of the component accurately reflects the condition of the component and the decision to trip or not to trip the component is based on the condition of the component irrespectively of the parameter of condition of other system components. Figure 2 illustrates this concept. The proposed method requires a monitoring system of the component under protection that continuously measures terminal data (such as the terminal voltage magnitude and angle, the frequency, and the rate of frequency change) and component status data (such as the tap setting and the temperature). The dynamic state estimation processes these measurement data and extracts the real time dynamic model of the component and its operating conditions. It is clarified that the rate of frequency change is computed by using data from at least two consecutive cycles. Specifically, at each cycle the frequency of the system is computed by processing all the captured waveforms at that cycle. By comparing this value to the frequency value of the precious cycle the rate of frequency change is computed.

After estimating the operating conditions, the well-known chi-square test calculates the probability that the measurement data are consistent with the component model (see Figure 2). In other words, this probability, which indicates the confidence level of the goodness of fit of the component model to the measurements, can be used to assess the health of the transformer. The high confidence level indicates a good fit between the measurements and the model, which indicates that the operating condition of the component is normal. However, if the component has internal faults, the confidence level would be almost zero (i.e., the very poor fit between the measurement and the transformer model).

In general, the proposed method can identify any internal abnormality of the component within a cycle and trip the circuit breaker immediately. It is emphasized that the proposed dynamic state estimation based protection scheme is a generalization of differential protection. For this reason any internal fault in the protected zone will immediately detected by the proposed scheme - the same fast way as an internal fault is detected by a differential protection scheme. Furthermore, it does not degrade the security because arelay does not trip in the event of normal behavior of the component, for example inrush currents or over excitation currents in case of transformers, since in these cases the method produces a high confidence level that the normal behavior of the component is consistent with the model of the component. Note also that the method does not require any settings or any coordination with other relays.

While the proposed scheme can be viewed as a generalization of differential protection, its reliability is much better than differential protection. As an example while line to line internal faults cannot be detected by differential schemes, the proposed dynamic state estimation protection does detect line to line internal faults immediately.

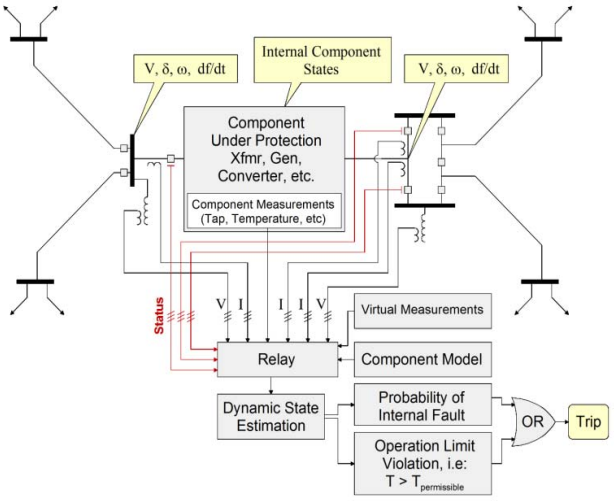

Figure 2: Illustration of setting-less component protection scheme

4. Implementation of Setting-less Protection

The implementation of the setting-less protection [9] has been approached from an object orientation point of view. For this purpose the constituent parts of the approach have been evaluated and have been abstracted into a number of objects. Specifically, the setting-less approach requires the following objects:

mathematical model of the protection zone
physical measurements of analog and digital data
mathematical model of the physical measurements
mathematical model of the virtual measurements
mathematical model of the derived measurements
mathematical model of the pseudo measurements
dynamic state estimation algorithms
bad data detection and identification algorithm
protection logic and trip signals
online parameter identification method

The last task is fundamental for model verification and fine tuning the parameters of the

models. It is done via online parameter identification methods. Conceptually the method is very simple. When a disturbance occurs the dynamic state estimation process is modified by treating selected parameters of the model as unknowns in the estimation process. The resulting solution of the dynamic state estimation provides better estimates of the parameters of the zone. The overall process is shown in Figure 3.

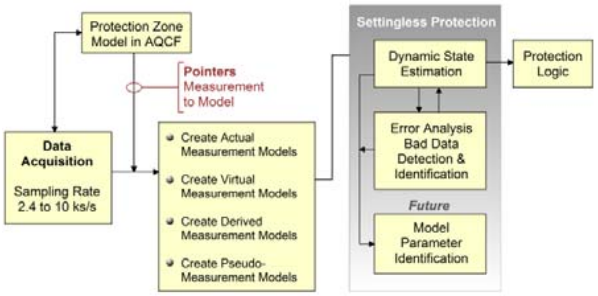

Figure 3: Setting-less protection relay organization

The details of this protection approach can be found in [9]. Several user interfaces have been developed to visualize the operation of these relays. Figure 4 illustrates an example. The example shows the visualization of the setting-less protection for a transformer; the terminal voltages and currents are shown in real time as well as the results of the chi-square test and the trip no-trip decision.

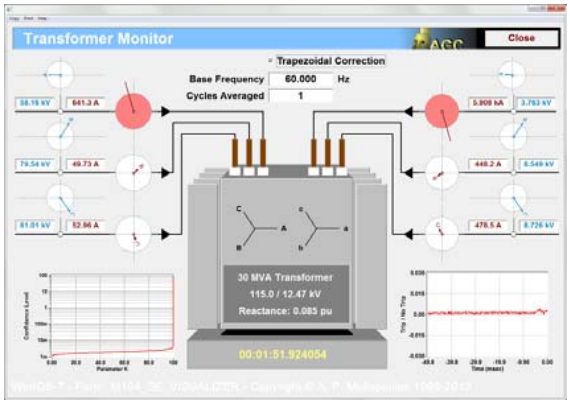

Figure 4: Visualization of transformer setting-less protection

5. Model Parameter Identification

The modeling issue is fundamental in this approach. For success the model must be high fidelity so that the component state estimator will reliably determine the operating status (health) of the component. For example consider a transformer during energization. The transformer will experience high in-rush current that represent a tolerable operating condition and therefore no relay action should occur. The component state estimator should be able to "track" the in-rush current and determine that they represent a tolerable operating condition. This requires a transformer model that accurately models saturation and in-rush current in the transformer. The transformer model is a good example of nonlinear model with controls and the general modeling approach for a transformer is given in Appendix A.

For many power system components, high fidelity models exist. For some newer components such as inverter interfaced power components, the modeling accuracy may not be as high. In both cases the state estimation process can be utilized the fine tune the models and/or determine the parameters of the model with greater accuracy. These procedures have been demonstrated in [12]. The basic approach is to expand the dynamic state estimator to include as parameters to be estimated some key model parameters. Therefore the overall approach can also provide better models with field validated parameters.

We can foresee the possibility that a high fidelity model used for protective relaying can be used as the main depository of the model which can provide the appropriate model for other applications. For example for EMS applications, a positive sequence model can be computed from the high fidelity model and send to the EMS data base. The advantage of this approach will be that the EMS model will come from a field validated model (the utilization of the model by the relay in real time provide the validation of the model). This overall approach is shown in Figure 5.

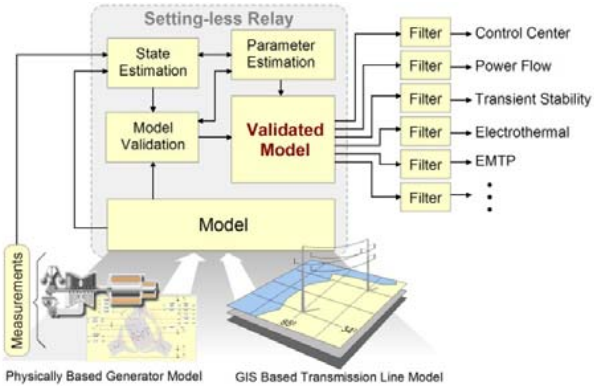

Figure 5: Illustration of setting-less protection logic

Since protection is ubiquitous, it makes economic sense to use relays for distributed model data base that provides the capability of perpetual model validation.

6. Substation Model Synthesis

The results of the dynamic state estimation over a period of one cycle are in the time domain. Specifically, the point on wave data is available for each variable of the zone under protection. This data are converted into the frequency domain by applying Fourier transform on the time domain data over a user specified time interval, for example one cycle. Because the frequency of the system may vary in real time, the Fourier transform must estimate the frequency first and then perform the Fourier analysis. Otherwise issues of spectral leakage may appear. We have developed a generalized approach for the computation of the phasors that provide high accuracy in phasor computation under varying frequency and waveform distortion. We refer to this method as the "Standard PMU". The standard PMU is the subject of a paper to be released in the near future. The end result of these computations is the zone model in frequency domain. The over organization is shown in Figure 6.

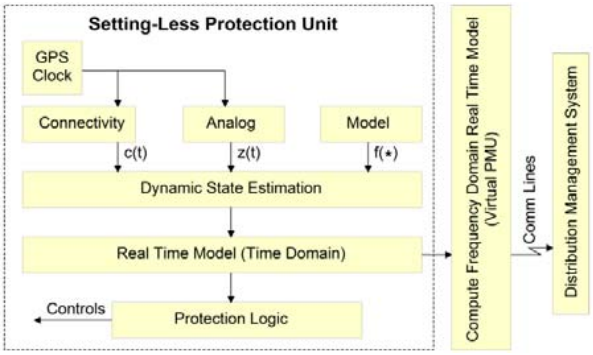

Figure 6: Functional diagram of setting-less protection unit

The phasor model is expressed in terms of four sets of data: ((1) connectivity, (2) device model, (3) measurements, and (4) controls). Each phasor model has also a time tag, the time at which this model is valid. Subsequently, this information is used to synthesize the substation state estimate. This process is quite simple: the state estimates of each zone are aligned by the time stamp. The zone models of a specific time stamp are collected to form the substation state estimate. In our work we use a time interval of one cycle and therefore the substation state estimate is updated once per cycle. Finally the substation state is transmitted to the control center where the system state is synthesized. Note that the synthesis of the substation state does not require additional computations since the component models are all in UTC time (due to the GPS synchronized measurements) and therefore they can be simply merged to provide the substation model.

7. System Wide Model Synthesis

The substation state estimate (in frequency domain) is used to directly synthesize the state of the entire system. This process is similar to the synthesis of the substation state estimate with the only difference that since the substation states are already in frequency domain this synthesis is straightforward and does not require any model conversions. The synthesis of the system wide state estimate is illustrated in Figure 7. Figure 7 illustrates how the EMS synthesizes the system wide model from substation state estimates. Each component's connectivity data is used to compose the topology of the substation. Using that topology, state estimates from each component that have the same GPS time stamp are immediately combined (with no additional calculations) to obtain the system wide state estimate.

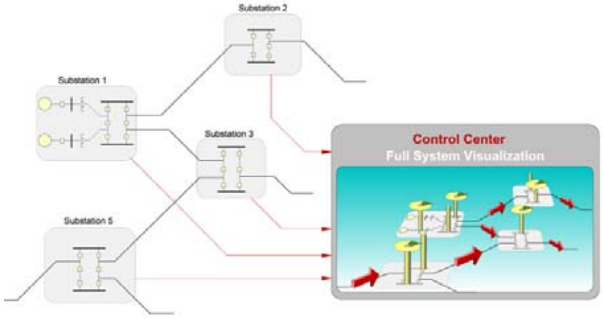

Figure 7: Synthesis of system wide state estimate from substation state estimates

8. Applications

The proposed infrastructure provides the real time model of the system across the spatial extend of the system. The real time model of components (zones), substation and system wide is available in an autonomous manner. This model is high fidelity and can be converted into other models of lower accuracy, such as models for load flow analysis. We have seen that the results of the dynamic state estimation are used directly for the protection of the particular zone. The real time model can be used for a variety of other applications. Several examples can be discussed. Because of space limitations we discuss the important application of optimal power flow (OPF).

Note that the phasor model discussed in section 6 includes the following four sets of data: ((1) connectivity, (2) device model, (3) measurements,

and (4) controls). The phasor model is organized into an object with specific structure. We refer to this structure as the state and control algebraic quadratic companion form (SCAQCF) [10-12]. We discuss here the autonomous formulation of the optimal power flow and its solution by simply using the object oriented component model.

Each component model is expressed with:

$$I(\mathbf{x},\mathbf{u}) = Y_{eqx}\mathbf{x} + \begin{Bmatrix} \vdots \\ \mathbf{x}^T F^i_{eqx} \mathbf{x} \\ \vdots \end{Bmatrix} + Y_{equ}\mathbf{u} + \begin{Bmatrix} \vdots \\ \mathbf{u}^T F^i_{equ} \mathbf{u} \\ \vdots \end{Bmatrix} + \begin{Bmatrix} \vdots \\ \mathbf{x}^T F^i_{eqxu} \mathbf{u} \\ \vdots \end{Bmatrix} - B_{eq} \quad (1)$$

$$\mathbf{y}(\mathbf{x},\mathbf{u}) = Y_{m,x}\mathbf{x} + \begin{Bmatrix} \vdots \\ \mathbf{x}^T F^i_{m,x} \mathbf{x} \\ \vdots \end{Bmatrix} + Y_{m,u}\mathbf{u} + \begin{Bmatrix} \vdots \\ \mathbf{u}^T F^i_{m,u} \mathbf{u} \\ \vdots \end{Bmatrix} + \begin{Bmatrix} \vdots \\ \mathbf{x}^T F^i_{m,xu} \mathbf{u} \\ \vdots \end{Bmatrix} + C_m \quad (2)$$

where:

$I(\mathbf{x},\mathbf{u})$: the through variables of the device model.

$\mathbf{x}$: external and internal state variables of the device model,

$\mathbf{u}$:the control variables of the device model.

Y_{eqx} : matrix defining the linear part for state variables.

F_{eqx} :matrices defining the quadratic part for state variables.

Y_{equ} :matrix defining the linear part for control variables.

F_{equ} :matrices defining the quadratic part for control variables.

B_{eq} : constant vector of the device model.

Above equations, connectivity data, and control data are utilized to autonomously formulate and solve the optimal power flow as discussed below.

The mathematical formulation of the optimal power flow problem is as follows:

$$\begin{aligned} &\min\ \mu\sum\left(\left|\mathbf{I}_m\right|\right) + f(\mathbf{x},\mathbf{u}) \\ &s.t.\ \ \mathbf{g}(\mathbf{x},\mathbf{u}) = 0 \\ &\qquad \mathbf{h}^{\min} \le \mathbf{h}(\mathbf{x},\mathbf{u}) \le \mathbf{h}^{\max} \\ &\qquad \mathbf{u}^{\min} \le \mathbf{u} \le \mathbf{u}^{\max} \end{aligned} \quad (3)$$

Where $\mathbf{I}_m$ is the mismatch variable vector, $\mathbf{x}$ is the state variable vector, and $\mathbf{u}$ is the control variable vector. In the objective function, μ is the penalty factor and f($\mathbf{x}$, $\mathbf{u}$) is the cost function, which can be the sum of the voltage deviations at each bus.

$\mathbf{g}(\mathbf{x}, \mathbf{u}) = 0$ are power flow equations, and they are created by collecting the connectivity data of each component which is described previously and applying KCL at each node of the network and adding the internal model equations of all components, assuming that the control variables have a fixed value.

$$\mathbf{g}(\mathbf{x},\mathbf{u}) = \begin{cases} \sum_{j\in N(i)} I_{ji} = 0 \ \ for\ all\ the\ nodes \\ Internal\ equations\ of\ all\ devices \end{cases} \quad (4)$$

Where N(i) is the set of nodes connected to i. In the above equations, all the currents are substituted with the appropriate equation from the component SCAQCF model equations yielding a set of equations in terms of the state variables only. This is a synthesis procedure that combines the validated high fidelity real time model of all the components extracted from the setting-less protection.

$h_{min} \le h(\mathbf{x}, \mathbf{u}) \le h_{max}$ are operating constraints, which include the upper and lower bounds for the voltage magnitudes at bus k and capacity constraints for transmission lines and transformers. For each lines and transformers of the system, the capacity constraints can be extracted from the SCAQCF component model as:

$$\left(I^{\min}_{mag}\right)^2 \le \begin{Bmatrix} \sum_i \sum_j Y^{2k}_{eqx,i} x_i x_j + \sum_i \sum_j Y^{2k+1}_{eqx,i} x_i x_j \\ -\sum_i Y^{2k}_{eqx,i} B_{eq,2k} x_i - \sum_i Y^{2k+1}_{eqx,i} B_{eq,2k+1} x_i \\ +B^2_{eq,2k} + B^2_{eq,2k+1} \end{Bmatrix} \le \left(I^{\max}_{mag}\right)^2 \quad (5)$$

Where the subscript k represents the terminal k of the SCAQCF component model and $Y^{2k}_{eq,x,i}$ represents the i-th element of the 2k-th row of the matrix $Y_{eq,x}$ and so on.

$u_{min} \le u \le u_{max}$ are control variable bounds.

The main advantage of the utilization of the proposed SCAQCF model is that it enables the automatic synthesis of the OPF problem as well as its solution. Any new resource of component added to the system will be automatically accounted in the optimization as long as its model is presented in the SCAQCF syntax. Also note that by virtue of the quadratic structure of the SCAQCF model, all the analytics of the optimization problem are in terms of quadratic equations.

The solution method for the OPF problem is based on barrier method. The algorithm first converts the OPF to a linearized optimization problem with only control variables using the co-state method. And the constraints contain power flow equations and operational constraints. Control variables are limited

by their physical bounds. The algorithm then obtains the updated values of control variable using barrier method and state variable by updating the power flow. If some modeled operational constraints are violated, the constraint will be updated in the linearized optimization problem and the previous solution is retrieved. If some other constraints are violated, the algorithm adds these constraints, retrieves the previous solution, and linearizes the new constraints. If mismatch variables are nonzero, the next iteration starts and variables may be reclassified.

It is emphasized that the object-oriented SCAQCF component model enables the solution for the OPF problem, autonomously, regardless of different types and features of the components in the system. Here we present one specific computational task of the OPF as an example: the task of linearization of the OPF problem. First both the objective function and the constraints of the OPF problem can be expressed in the following generic quadratic form (these equations are provided by the SCAQCF):

$$J(\mathbf{x},\mathbf{u}) = A_J \cdot \mathbf{x} + \mathbf{x}^T \cdot B_J \cdot \mathbf{x} + D_J \cdot \mathbf{u} + \mathbf{u}^T \cdot E_J \cdot \mathbf{u} + \mathbf{x}^T \cdot F_J \cdot \mathbf{u} + c \quad (6)$$

Where A_J, B_J, D_J, E_J and F_J represent the linear part of state, quadratic part of state, linear part of control variable, quadratic part of control variable and quadratic part of state and control variable respectively.

The linearization step eliminates the state variables and re-casts the optimization problem, expressing it only in terms of control variables [13]. This step uses the co-state method to obtain the linearized forms of all functions. The formula to compute the coefficients of all control variables is:

$$\frac{dJ(\mathbf{x}^o,\mathbf{u}^o)}{d\mathbf{u}} = \frac{\partial J(\mathbf{x}^o,\mathbf{u}^o)}{\partial \mathbf{u}} - \hat{\mathbf{x}}^T \frac{\partial \mathbf{g}(\mathbf{x}^o,\mathbf{u}^o)}{\partial \mathbf{u}} \quad (7)$$

$$\text{Where } \hat{\mathbf{x}}^T = \frac{\partial J_k(\mathbf{x}^o,\mathbf{u}^o)}{\partial \mathbf{x}} \left(\frac{\partial \mathbf{g}(\mathbf{x}^o,\mathbf{u}^o)}{\partial \mathbf{x}} \right)^{-1} \quad (8)$$

Based on the SCAQCF model and the generic form of the object function and constraint, each term in equations (7-9) is automatically computed as follows,

$$\frac{\partial \mathbf{g}(\mathbf{x}^o,\mathbf{u}^o)}{\partial \mathbf{u}} = Y_{equ} + \left\{ \mathbf{u}^{o,T} F_{equ,i} \right\} + \left\{ \left(F_{equ,i} \mathbf{u}^o \right)^T \right\} + \left\{ \mathbf{x}^{o,T} F_{eqxu,i} \right\} \quad (9)$$

$$\frac{\partial J(\mathbf{x}^o,\mathbf{u}^o)}{\partial \mathbf{x}} = A_J + \mathbf{x}^{o,T} \cdot B_J + \left(B_J \cdot \mathbf{x}^o \right)^T + \left(F_J \cdot \mathbf{u}^o \right)^T \quad (10)$$

$$\frac{\partial J(\mathbf{x}^o,\mathbf{u}^o)}{\partial \mathbf{u}} = D_J + \mathbf{u}^{o,T} \cdot E_J + \left(E_J \cdot \mathbf{u}^o \right)^T + \mathbf{x}^{o,T} \cdot F_J \quad (11)$$

$$\frac{\partial \mathbf{g}(\mathbf{x}^o,\mathbf{u}^o)}{\partial \mathbf{x}} = Y_{eqx} + \left\{ \mathbf{x}^{o,T} F_{eqx,i} \right\} + \left\{ \left(F_{eqx,i} \mathbf{x}^o \right)^T \right\} + \left\{ \left(F_{eqxu,i} \mathbf{u}^o \right)^T \right\} \quad (12)$$

The proposed method was tested to determine the optimal active and reactive dispatch in the IEEE 30 bus system, shown in Figure 8. For this application each component of the IEEE 30 bus system was converted into the SCAQCF. Subsequently the OPF problem was autonomously formulated and solved. The system was loaded heavily, to demonstrate how the approach is able to correctly handle line ratings and generator active and reactive limits. Subsequently, a 10 MVA Wind Farm was added at bus 8, to demonstrate how the object oriented approach is able to handle this new resource and incorporate its capabilities to the OPF problem (autonomously), thus reaching a better optimal operating point. For illustrative purposes, it is assumed that the power output of this wind farm is 0 MW, thus it is able to support the system with reactive power injection of up to 10 MVAr from its power electronics converter.

The maximum allowable bus voltage in this solution is 1.05 pu and the minimum is 0.95. The OPF solution results for the base case are summarized in Tables 1-6.

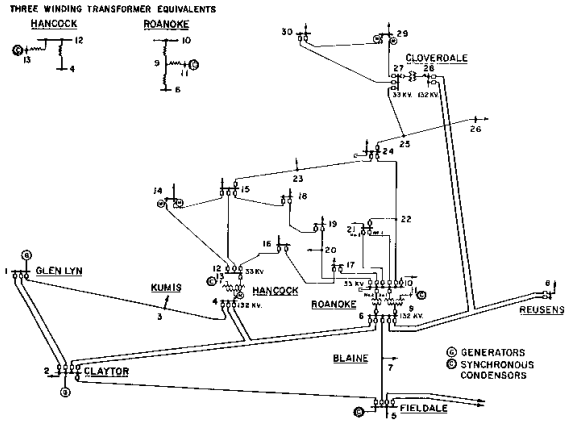

Figure 8: The IEEE 30 bus system

Table 1: OPF system results summary

Overall Cost ($/hr)	603.81
Available Generation (MW)	335
Actual Generation (MW)	218.3
Load (MW)	213.2
Active Losses (MW)	5.1
Reactive Generation (MVAr)	126.6
Reactive Load (Mvar)	119.8

Table 2: OPF generator dispatch summary

Generator Bus	P (MW)	Q (MVAr)	Marginal Cost ($/MWr)
1	80	-7.35	3.151
2	41.66	-5.52	3.208

13	11.34	44.7	3.567
22	21.01	32.38	3.627
23	16.28	15.89	3.814
27	48	46.47	4.051

Table 3: OPF generator active voltage constraints summary

Bus	V (pu)	V_{min}(pu)	V_{max}(pu)
7	0.95	0.95	1.05
25	1.05	0.95	1.05

Table 4: OPF active PG constraints summary

Generator #	Bus #	P_G (MW)	$P_{G,max}$ (MW)
1	1	80	80

Table 5: OPF active QG constraints summary

Generator #	Bus #	Q_G (MVAr)	$Q_{G,max}$ (MVAr)
6	13	44.7	44.7

Table 6: OPF activeline rating constraints summary

From	To	Apprarent Power Flow (MVA)	Line Rating (MVA)
6	8	32	32
22	21	32	32
27	25	16	16

When the 10MVA wind farm at bus 8 is connected, the model of the system is updated, and the new object of component, in this case a converter interfaced wind farm is automatically synthesized within the system wide model. The OPF is resolved, and the reactive support capabilities of the wind farm's converter yield a better optimal solution. The OPF results with the wind farm connected are summarized in tables 7-11.

Table 7: OPF system results summary

Overall Cost ($/hr)	593.56
Available Generation (MW)	335
Actual Generation (MW)	217.5
Load (MW)	213.2
Active Losses (MW)	4.29
Reactive Generation (MVAr)	117.2
Reactive Load (Mvar)	119.8

Table 8: OPF generator dispatch summary

Generator Bus	P (MW)	Q (MVAr)	Marginal Cost ($/MWr)
1	80	-6.95	3.603
2	54.64	21.43	3.662
8	0	10	-
13	15.37	29.8	3.769
22	22.26	27.88	3.783
23	15.15	6.79	3.757
27	30.06	28.26	3.751

Table 9: OPF active voltage constraints summary

Bus	V (pu)	V_{min}(pu)	V_{max}(pu)
1	1.05	0.95	1.05
12	1.05	0.95	1.05
25	1.05	0.95	1.05

Table 10: OPF active PG constraints summary

Generator #	Bus #	P_G (MW)	$P_{G,max}$ (MW)
1	1	80	80

Table 11: OPF active QG constraints summary

Generator #	Bus #	Q_G (MVAr)	$Q_{G,max}$ (MVAr)
7	8	10	10

The 10MVAr reactive support capabilities of the wind farm are fully utilized. The OPF solution yields no active line rating constraints, thus the synthesis of the wind farm to the system model indeed allows decongestion of the system's lines. Furthermore, the overall cost and active power losses are reduced and no low bus voltage constraints are active.

In conclusion, the autonomous optimal power flow illustrates the capability of the proposed infrastructure to provide the basis for seamless applications. The implementation of this approach requires that the real time model in the standard object oriented description be send to the control center where the optimal power flow problem is autonomously formed and solved. It is emphasized that the nonlinear OPF problem is solved subject to the constraints of the system and the controls. While only the OPF application has been discussed, it is important to state that any control center application can be similarly implemented in a seamless fashion.

9. Conclusion

The proposed infrastructure enables a fully autonomous monitoring, protection and operation of a wide area system. The approach is based on equipping the basic data acquisition systems with intelligence to collect not only data but also the component model as well as the connectivity and controls of the component. GPS time synchronization is a requirement of the approach since the analytics require that the derived models and state estimates be time stamped with accuracy of microseconds.

The basic concept and objectives of the smart grid and grid modernization is to utilize existing and future technologies for the purpose of increasing the level of automation and autonomy of the power system of the future. Towards this goal it is important to remove human intervention or needs for human input as much as possible to avoid possibilities of

human error as the operation of the system becomes more complex and the number of players is increasing. We have proposed an infrastructure that practically eliminates human input in the process of extracting the real time model of the system and using the real time model for (a) protection and (b) model based optimization and control. The real time model is available across the spatial extend of the electric power system. The infrastructure is based on the capabilities of present day high end numerical relays. The technology required for the implementation of the proposed scheme exists today.

10. Acknowledgement

The work in this paper was partially supported by the EPRI (Power System Engineering Research Center project T-49G),and DoE/NETL project DE-OE0000117.Their support of this work is gratefully acknowledged.

11. References

[1] A. P. Sakis Meliopoulos, Anjan Bose, PSERC Publication 10-17, *Substation of the Future: A Feasibility Study*, October 2010.

[2] B. Kasztenny, J. Schaefer, and E. Clark, "Fundamentals of adaptive protection of large capacitor banks - accurate methods for canceling inherent bank unbalances," in *Proc. 60th Annual Conference for Protective Relay Engineers*, Mar. 2007, pp. 126-157.

[3] E. Farantatos, G. K. Stefopoulos, G. J. Cokkinides, and A. P. S. Meliopoulos, "PMU-based dynamic state estimation for electric power systems," in *Proc. IEEE PES General Meeting*, Jul. 2009

[4] R. Huang, E. Farantatos, G. J. Cokkinides, and A. P. S. Meliopoulos, "Substation based dynamic state estimator - numerical experiment," in *Proc. IEEE PES Transmission and Distribution Conference and Exposition*, New Orleans, Apr. 2010.

[5] A. P. S. Meliopoulos, G. J. Cokkinides, F. Galvan, B. Fardeanesh, and P. Myrda, "Delivering accurate and timely data to all," *IEEE Power and Energy Magazine,* vol. 5, no. 3, pp. 74-86, May 2007.

[6] A. P. S. Meliopoulos, G. J. Cokkinides, C. Hedrington, and T. L. Conrad, "The supercalibrator - a fully distributed state estimator," in *Proc. IEEE PES General Meeting*, Jul. 2010.

[7] A. P. Meliopoulos, G. J. Cokkinides, and G. K. Stefopoulos, "Improved numerical integration method for power/power electronic systems based on three-point collocation," in *Proc. the 44th IEEE Conference on Decision and Control, and European Control Conference*, Dec. 2005, pp. 6780-6787.

[8] Sungyun Choi, Beungjin Kim, George Cokkinides and A. P. Sakis Meliopoulos, "Feasibility Study: Autonomous State Estimation in Distribution Systems", *IEEE Transactions on Power Systems*, Vol. 26, No. 4, pp 2109-2117, November 2011

[9] A. P. Sakis Meliopoulos, George Cokkinides, Zhenyu Tan, Sungyun Choi, Yonghee Lee, and Paul Myrda, "Setting-less Protection: Feasibility Study", *Proceedings of the of the 46st Annual Hawaii International Conference on System Sciences*, Maui, HI, January 7-10, 2013.

[10] A. P. S. Meliopoulos, G. J. Cokkinides, and G. Stefopoulos, "Quadratic integration method," in *Proc. International Power System Transients Conference*, Montreal, Jun. 2005.

[11] G. Stefopoulos, G. J. Cokkinides, and A. P. S. Meliopoulos, "Expert symbolic transient simulator based on quadratic integration method," in *Proc. the 13th International Conference on Intelligent Systems Application to Power Systems*, Nov. 2005, pp. 347-353.

[12] G. K. Stefopoulos, G. J. Cokkinides, and A. P. S. Meliopoulos, "Quadratized model of nonlinear saturable-core inductor for time-domain simulation," in *Proc. IEEE PES General Meeting*, Jul. 2009.

[13] Y. Tao and A. P. Meliopoulos, "Optimal power flow via quadratic power flow," in *Proceedings of Power Systems Conference and Exposition*, Mar. 20-23 2011, pp. 1-8

Appendix A: Single Phase Transformer Model for Setting-less Protection

This Appendix provides an example of a SCAQCF model. The example is selected so that it demonstrates the handling of non-linearities, controls and limits and at the same time should be simple so that it can fit in the constraints of the paper. This example is a single phase saturable core variable tap transformer. The model is first presented with what we call the compact form, which is the familiar standard notation model. We subsequently quadratize the model and then the quadratic model is integrated to provide the SCAQCF model.

Figure A1 gives the model of the single phase transformer. In Figure A1, the turn ratio t consists of two parts. One is the nominal transformation ratio t_n, which in the model is treated as a fixed constant and the other is the per-unit tap selection t_u, which in the model is treated as a controllable variable. The overall turn ratio is $t = t_u t_n$. And the resistance r_1, inductance L_1 at the primary side and the resistance r_2, inductance L_2 at the secondary side are expressed as follows:

$$r_1 = 2t_n^2 r, L_1 = 2t_n^2 L$$

$$r_2 = \frac{2r}{1-|1-t_u|}, L_2 = \frac{2L}{1-|1-t_u|}$$

where r and L are the nominal resistance and inductance of the transformer referred to the secondary side.

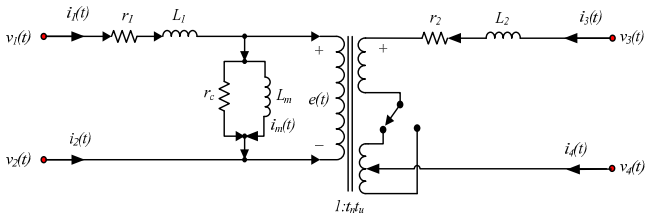

Figure A-1: The single phase transformer model

The compact model of the single phase saturable core variable tap transformer of Figure A1 is:

$$v_1(t) - v_2(t) = 2t_n^2 r i_{1L}(t) + 2t_n^2 L \frac{d}{dt} i_{1L}(t) + e(t)$$

$$v_3(t) - v_4(t) = \frac{2r}{1-|1-t_u(t)|} i_{3L}(t) + \frac{2L}{1-|1-t_u(t)|} \frac{d}{dt} i_{3L}(t) + t_n t_u(t) e(t)$$

$$r_c\, i_{1L}(t) + r_c t_n t_u(t)\, i_{3L}(t) = e(t) + r_c i_m(t)$$

$$e(t) = \frac{d}{dt}\lambda(t)$$

$$i_m(t) - i_0 \left| \frac{\lambda(t)}{\lambda_0} \right|^n sign(\lambda(t)) = 0$$

$$0.9 < t_u(t) < 1.1$$

Where $v_1(t)$, $v_2(t)$, $v_3(t)$, $v_4(t)$, $i_1(t)$, $i_2(t)$, $i_3(t)$ and $i_4(t)$ are the terminal voltages and currents respectively. $i_{1L}(t)$ and $i_{3L}(t)$ are the currents through the inductance L_1 and L_2 and $i_m(t)$ are the magnetizing current. Note that the model is linear except the magnetization equation that in general is quite non-linear and the tap control variable appears in absolute value. The exponent n in general a number between 9 and 13 depending on core material. The exponent n is determined by the manufacturer magnetization curve if available or it can be derived from the magnetizing current versus voltage if this information is available. The above model is quadratized, i.e. all non-linearities above 2 are converted into equations with maximum exponent of 2 by introducing more state variables. In order to limit the complexity of the example we will assume that n=5. Also the tap control variable appears in absolute value is quadratized by introducing new state variables as:

$$u_1(t) = \sqrt{(1-t_u(t))^2}$$

$$u_2(t) = \frac{1}{1+u_1(t)}$$

The quadratized model is:

$$i_1(t) = i_{1L}(t)$$

$$i_2(t) = -i_{1L}(t)$$

$$i_3(t) = i_{3L}(t)$$

$$i_4(t) = -i_{3L}(t)$$

$$0 = v_1(t) - v_2(t) - e(t) - 2t_n^2 r i_{1L}(t) - 2t_n^2 L z_1(t)$$

$$0 = v_3(t) - v_4(t) - t_n t_u(t)\, e(t) - 2r u_2(t) i_{3L}(t) - 2L u_2(t) z_2(t)$$

$$0 = r_c\, i_{1L}(t) + r_c t_n t_u(t)\, i_{3L}(t) - e(t) - r_c i_m(t)$$

$$0 = e(t) - \frac{d}{dt}\lambda(t)$$

$$0 = \frac{d}{dt} i_{1L}(t) - z_1(t)$$

$$0 = \frac{d}{dt} i_{3L}(t) - z_2(t)$$

$$0 = t_u^2(t) + u_1^2(t) - 1$$

$$0 = u_1(t) u_2(t) + u_2(t) - 1$$

$$0 = y_1(t) - \left(\frac{\lambda(t)}{\lambda_0} \right)^2$$

$$0 = y_2(t) - y_1^2(t)$$

$$0 = i_m(t) - \frac{i_0}{\lambda_0} y_2(t) \lambda(t)$$

$$0.9 < t_u(t) < 1.1$$

Where the state variables are

$$X = \begin{bmatrix} v_1(t), v_2(t), v_3(t), v_4(t), i_{1L}(t), i_{3L}(t), e(t), \lambda(t), \\ i_m(t), z_1(t), z_2(t), y_1(t), y_2(t), u_1(t), u_2(t), \end{bmatrix}$$

the through variables are

$$I = [i_1(t), i_2(t), i_3(t), i_4(t)]$$

and the control variable is

$$U = [t_u(t)]$$

The differential equations in above model are integrated with the quadratic integration method[10-11] and the equations that are algebraic are sufficed to be written at times t and t_m. And this quadratic integration procedure yielding the following model.

$$i_1(t) = i_{1L}(t)$$

$$i_2(t) = -i_{1L}(t)$$

$$i_3(t) = i_{3L}(t)$$

$$i_4(t) = -i_{3L}(t)$$

$$0 = v_1(t) - v_2(t) - e(t) - 2t_n^2 r i_{1L}(t) - 2t_n^2 L z_1(t)$$

$$0 = v_3(t) - v_4(t) - t_n t_u(t)\, e(t) - 2r u_2(t) i_{3L}(t) - 2L u_2(t) z_2(t)$$

$$0 = r_c\, i_{1L}(t) + r_c t_n t_u(t)\, i_{3L}(t) - e(t) - r_c i_m(t)$$

$$0 = t_u^2(t) + u_1^2(t) - 1$$

$$0 = u_1(t)u_2(t) + u_2(t) - 1$$
$$0 = y_1(t) - \left(\frac{\lambda(t)}{\lambda_0}\right)^2$$
$$0 = y_2(t) - y_1^2(t)$$
$$0 = i_m(t) - \frac{i_0}{\lambda_0} y_2(t)\lambda(t)$$
$$0 = \frac{h}{6}e(t) + \frac{2h}{3}e(t_m) - \lambda(t) + \left(\frac{h}{6}e(t-h) + \lambda(t-h)\right)$$
$$0 = \frac{h}{6}z_1(t) + \frac{2h}{3}z_1(t_m) - i_{1L}(t) + \left(\frac{h}{6}z_1(t-h) + i_{1L}(t-h)\right)$$
$$0 = \frac{h}{6}z_2(t) + \frac{2h}{3}z_2(t_m) - i_{3L}(t) + \left(\frac{h}{6}z_2(t-h) + i_{3L}(t-h)\right)$$
$$0.9 < t_u(t) < 1.1$$
$$i_1(t_m) = i_{1L}(t_m)$$
$$i_2(t_m) = -i_{1L}(t_m)$$
$$i_3(t_m) = i_{3L}(t_m)$$
$$i_4(t_m) = -i_{3L}(t_m)$$
$$0 = v_1(t_m) - v_2(t_m) - e(t_m) - 2t_n^2 r i_{1L}(t_m) - 2t_n^2 L z_1(t_m)$$
$$0 = v_3(t_m) - v_4(t_m) - t_n t_u(t_m) e(t_m) - 2r u_2(t_m) i_{3L}(t_m) - 2L u_2(t_m) z_2(t_m)$$
$$0 = r_c\, i_{1L}(t_m) + r_c t_n t_u(t_m) i_{3L}(t_m) - e(t_m) - r_c i_m(t_m)$$
$$0 = t_u^2(t_m) + u_1^2(t_m) - 1$$
$$0 = u_1(t_m)u_2(t_m) + u_2(t_m) - 1$$
$$0 = y_1(t_m) - \left(\frac{\lambda(t_m)}{\lambda_0}\right)^2$$
$$0 = y_2(t_m) - y_1^2(t_m)$$
$$0 = i_m(t_m) - \frac{i_0}{\lambda_0} y_2(t_m)\lambda(t_m)$$
$$0 = -\frac{h}{24}e(t) + \frac{h}{3}e(t_m) - \lambda(t) + \left(\frac{5h}{24}e(t-h) + \lambda(t-h)\right)$$
$$0 = -\frac{h}{24}z_1(t_m) + \frac{h}{3}z_1(t_m) - i_{1L}(t) + \left(\frac{5h}{24}z_1(t-h) + i_{1L}(t-h)\right)$$
$$0 = -\frac{h}{24}z_2(t) + \frac{h}{3}z_2(t_m) - i_{3L}(t) + \left(\frac{5h}{24}z_2(t-h) + i_{3L}(t-h)\right)$$
$$0.9 < t_u(t_m) < 1.1$$

Note that the above model is in the SCAQCF form as indicated by equation (1). Due to the space limits, the various matrices in the SCAQCF equation for the above model are not provided here, but it is emphasized that by comparing the above model and equation (1), it is easy to define all the matrices in the SCAQCF form.

The measurement model in the same form is derived as follows. Assume that the measurements are:

1. Actual measurements, which are the voltage measurements $\tilde{v}_{12}^m(t)$, $\tilde{v}_{34}^m(t)$ and current measurements $\tilde{i}_1^m(t)$, $\tilde{i}_3^m(t)$.
2. Derived measurements, which are the current measurements $\tilde{i}_2^m(t)$, $\tilde{i}_4^m(t)$ at terminal 2 and 4 and they are supposed to have same absolute values as $\tilde{i}_1^m(t)$, $\tilde{i}_3^m(t)$ but a different direction.
3. Pseudo measurements, which are the measurements $\tilde{v}_2^m(t)$, $\tilde{v}_4^m(t)$, assuming voltages at terminals 2 and 4 are zero (Neutral voltages).
4. Virtual measurements, which are the internal equations with left side equals to zero in the transformer SCQACF form (totally 22 equations).

Each one of the above measurements is expressed in terms of the SCAQCF model, providing the measurement model is SCAQCF form:

$$\tilde{v}_{12}^m(t) = v_1(t) - v_2(t) + \eta$$
$$\tilde{v}_{34}^m(t) = v_3(t) - v_4(t) + \eta$$
$$\tilde{i}_1^m(t) = i_{1L}(t) + \eta$$
$$\tilde{i}_3^m(t) = i_{3L}(t) + \eta$$
$$\tilde{i}_2^m(t) = -i_{1L}(t) + \eta$$
$$\tilde{i}_4^m(t) = -i_{3L}(t) + \eta$$
$$\tilde{v}_2^m(t) = 0 + \eta$$
$$\tilde{v}_4^m(t) = 0 + \eta$$
$$0 = v_1(t) - v_2(t) - e(t) - 2t_n^2 r i_{1L}(t) - 2t_n^2 L z_1(t) + \eta$$
$$0 = v_3(t) - v_4(t) - t_n t_u(t) e(t) - 2r u_2(t) i_{3L}(t) - 2L u_2(t) z_2(t) + \eta$$
$$0 = r_c\, i_{1L}(t) + r_c t_n t_u(t) i_{3L}(t) - e(t) - r_c i_m(t) + \eta$$
$$0 = t_u^2(t) + u_1^2(t) - 1 + \eta$$
$$0 = u_1(t)u_2(t) + u_2(t) - 1 + \eta$$
$$0 = y_1(t) - \left(\frac{\lambda(t)}{\lambda_0}\right)^2 + \eta$$
$$0 = y_2(t) - y_1^2(t) + \eta$$
$$0 = i_m(t) - \frac{i_0}{\lambda_0} y_2(t)\lambda(t) + \eta$$
$$0 = \frac{h}{6}e(t) + \frac{2h}{3}e(t_m) - \lambda(t) + \left(\frac{h}{6}e(t-h) + \lambda(t-h)\right) + \eta$$
$$0 = \frac{h}{6}z_1(t) + \frac{2h}{3}z_1(t_m) - i_{1L}(t) + \left(\frac{h}{6}z_1(t-h) + i_{1L}(t-h)\right) + \eta$$
$$0 = \frac{h}{6}z_2(t) + \frac{2h}{3}z_2(t_m) - i_{3L}(t) + \left(\frac{h}{6}z_2(t-h) + i_{3L}(t-h)\right) + \eta$$
$$0 = v_1(t_m) - v_2(t_m) - e(t_m) - 2t_n^2 r i_{1L}(t_m) - 2t_n^2 L z_1(t_m) + \eta$$
$$0 = v_3(t_m) - v_4(t_m) - t_n t_u(t_m) e(t_m) - 2r u_2(t_m) i_{3L}(t_m) - 2L u_2(t_m) z_2(t_m) + \eta$$
$$0 = r_c\, i_{1L}(t_m) + r_c t_n t_u(t_m) i_{3L}(t_m) - e(t_m) - r_c i_m(t_m) + \eta$$

$$0 = t_u^2(t_m) + u_1^2(t_m) - 1 + \eta$$

$$0 = u_1(t_m)u_2(t_m) + u_2(t_m) - 1 + \eta$$

$$0 = y_1(t_m) - \left(\frac{\lambda(t_m)}{\lambda_0}\right)^2 + \eta$$

$$0 = y_2(t_m) - y_1^2(t_m) + \eta$$

$$0 = i_m(t_m) - \frac{i_0}{\lambda_0} y_2(t_m)\lambda(t_m) + \eta$$

$$0 = -\frac{h}{24}e(t) + \frac{h}{3}e(t_m) - \lambda(t) + \left(\frac{5h}{24}e(t-h) + \lambda(t-h)\right) + \eta$$

$$0 = -\frac{h}{24}z_1(t_m) + \frac{h}{3}z_1(t_m) - i_{1L}(t) + \left(\frac{5h}{24}z_1(t-h) + i_{1L}(t-h)\right) + \eta$$

$$0 = -\frac{h}{24}z_2(t) + \frac{h}{3}z_2(t_m) - i_{3L}(t) + \left(\frac{5h}{24}z_2(t-h) + i_{3L}(t-h)\right) + \eta$$

where η represents the measurement error. Note that the above measurement model is in the SCAQCF form as indicated by equation (2). Due to the space limits, the various matrices in the SCAQCF equation for the above measurement model are not provided here, but it is emphasized that by comparing the above measurement model and equation (2), it is easy to define all the matrices in the SCAQCF form.